(28) Sasaki, S.; Hikata, M.; Shiraki, C.; Uematsu, I. *Poly. J. (Tokyo)* **1982**, *14*, 205.
(29) Sasaki, S.; Tokuma, K.; Uematsu, I. *Polym. Bull. (Berlin)* **1983**, *10*, 539.
(30) Ginzburg, B.; Siromyatnikova, T.; Frenkel, S. *Polym. Bull. (Berlin)* **1985**, *13*, 139.
(31) Ferry, J. D *Viscoelastic Properties of Polymers*; Wiley: New York, 1961.
(32) Kiss, G.; Porter, R. S. *J. Polym. Sci., Polym. Symp.* **1978**, *No. 65*, 193.
(33) Aoki, H.; White, J. L.; Fellers, J. F. *J. Appl. Polym. Sci.* **1979**, *23*, 2293.
(34) Onogi, T.; Asada, T. *Rheology*, Astarita, G., Marucci, G., Nicolais, L., Eds.; Plenum: New York, 1980; Vol 1.
(35) Hermans, J. J. *J. Colloid. Sci.* **1962**, *17*, 638.
(36) Aharoni, S. M. *Polymer* **1980**, *21*, 1413.
(37) Iizuka, E. *Mol. Cryst. Liq. Cryst.* **1974**, *25*, 287.
(38) Miller, W. G.; Chakrabarty, S.; Seibel, K. M. *Microdomains in Polymer Solutions*; Dubin, P., Ed.; Plenum: New York, 1985; p 143.

Carrier Transport and Generation Processes in Polymer Electrolytes Based on Poly(ethylene oxide) Networks

Masayoshi Watanabe,* Masashi Itoh, Kohei Sanui, and Naoya Ogata

Department of Chemistry, Sophia University, Chiyoda-ku, Tokyo 102, Japan.
Received August 7, 1986

ABSTRACT: Carrier transport and generation processes were investigated in polymer electrolytes based on poly(ethylene oxide) networks in rubbery and amorphous states. The Williams–Landel–Ferry (WLF) plots of the ionic conductivity gave a master curve irrespective of the kinds of incorporated salts, and the WLF parameters obtained were comparable to the universal values for the relaxation times of many amorphous polymers. The ionic transport did not occur by itself; segmental motion with associated carrier ions caused the ionic transport. The ionic conductivity at constant reduced temperatures tended to decrease with increasing lattice energies of the incorporated salts. The increase in the conductivity as a function of the salt concentration at constant reduced temperatures was smaller than that expected by the complete dissociation of the salt. All of the incorporated salt did not function as carrier ions, and the ion dissociation was suppressed with increasing lattice energies and concentration of the salts.

Introduction

Solid solutions of salts in polymers are new kinds of electrolytes. Much interest has been focused on the high ionic conductivity of these polymer electrolytes in terms of a fundamental understanding of fast ion transport in polymers[1] and their potential application as solid electrolytes in primary or secondary high-energy-density batteries.[2,3]

Polymer complexes consisting of linear poly(ethylene oxide) (PEO) and alkali metal salts are prototypes of solvent-free polymer electrolytes.[4] The PEO complexes have, in general, multiphase nature, which consists of a salt-rich crystalline phase, a pure PEO crystalline phase, and an amorphous phase with dissolved salt. It has been revealed that the ionic conduction takes place primarily in the amorphous phase.[5] The phase diagram is affected by many factors, such as salt species and concentration, temperature, and preparative method. Thus, the ion-conducting behavior in PEO is complicated by the change in the phase diagram with the above factors.

Amorphous PEO–salt complexes permit the investigation of ion-conducting behavior in PEO without the complication of different phases. It has been pointed out that the temperature dependence of ionic conductivity for the amorphous PEO–salt complexes obeys a WLF type equation.[6,7] This fact indicates that the ion-transport process is correlated to the viscoelastic property of the host polymers.[6,7] However, what this fact means on the molecular level is still not clear. Furthermore, the WLF-type equation does not hold in the carrier generation process but holds in the carrier transport process. Since ionic conductivity is determined by the product of the number of carrier ions and their mobility, the carrier generation process will also affect the ionic conductivity. However, little is known about the carrier generation process, for example, little is known about the number of carrier ions as functions of the incorporated salt species and concentration, and temperature.[8]

In earlier articles[9,10] we investigated the ionic conductivity of PEO network polymers with dissolved lithium perchlorate. The network structure improved the conductivity of the salt complexes by decreasing considerably the degree of crystallinity. The purpose of this study is to investigate carrier transport and generation processes in PEO in completely amorphous and rubbery states. Various kinds of alkali metal salts were incorporated in the PEO network polymers. The WLF plots of the ionic conductivity gave a master curve irrespective of the kinds of incorporated salts. The ionic conductivities at constant reduced temperatures were correlated with the lattice energies and concentration of the salts.

Experimental Section

Materials. PEO triol having a number-average molecular weight of 3.0×10^3, which was determined by OH titration, was supplied by Dai-ichi Kogyo Seiyaku Co. The PEO triol was dried under reduced pressure (10^{-3} Torr) at 80 °C for 8 h just before use. A network polymer of PEO was prepared by reaction of the PEO triol with 4-methyl-1,3-phenylene diisocyanate at 80 °C for 96 h (as shown in Figure 1). With respect to the functional groups, stoichiometric amounts of the PEO triol and isocyanate were used for the reaction. The preparative method is described elsewhere.[10] Unreacted precursors were removed from the network polymers by extraction with acetone several times. After complete evaporation of the solvent, network polymer films of about 0.3-mm thickness were obtained. The sol fraction, which could be extracted by acetone, was lower than 1 wt %. IR spectra of the network polymers showed no absorption band at 2280 cm^{-1}, assignable to –NCO groups, and a trace absorption band around 3470 cm^{-1}, assignable to –OH groups. The resulting network polymers, having a favorable mechanical strength, were colorless and transparent elastomers at room temperature. The network polymers, which had the weight swelling ratio toward water of 2.7 ± 0.1 at 30 °C, were used for the preparation of polymer electrolytes.

Various kinds of alkali metal salts were dried at appropriate temperatures (>100 °C) under reduced pressure (10^{-3} Torr) for 8 h and kept under argon atmosphere just before use. The dissolution of alkali metal salts in the network polymers was per-

0024-9297/87/2220-0569$01.50/0

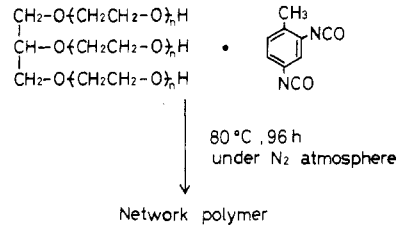

Figure 1. Preparation of PEO network polymers.

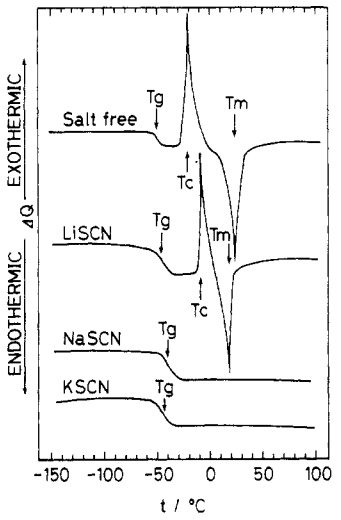

Figure 2. Profiles of DSC curves for salt-free PEO network polymer and PEO–alkali metal salt complexes.

formed by an immersion method using methanol or acetone solutions of the salts, as described elsewhere.[10,11] The concentration of the salts in the network polymers was determined from the weight change of the film before and after immersion, and the molar ratio of salt to the repeat unit of PEO ([salt]/[EO unit]) was 0.02, unless otherwise noted.

All handling of the PEO network polymer and the PEO–salt complexes was carried out under inert atmosphere in an argon-filled drybox in order to exclude traces of water.

Methods. The PEO–salt complexes sandwiched between platinum electrodes were subjected to complex impedance measurements. The frequency dependence of the cell impedance was measured with a Yokogawa-Hewlett-Packard 4192A LF-impedance analyzer. The ionic conductivity was determined from the complex impedance measurements. Details of the cell construction and the measurements are described elsewhere.[12] The temperature dependence of the ionic conductivity was measured with decreasing temperature after the temperature of the samples was raised to an upper limit for the measurements.

Differential scanning calorimetry (DSC) was carried out by using a Rigaku Denki 8058 DSC apparatus over the temperature range of −160 to 100 °C at a heating rate of 20 °C min^{-1}. The glass transition zone was determined as the temperature range of a heat capacity change during glass transition. The glass transition temperature (T_g) was defined as the midpoint of the heat capacity change. The enthalpy of crystallization (ΔH_c) and melting (ΔH_m) was estimated by using phenylazobenzene as a standard substance.

Results and Discussion

Temperature Dependence of Ionic Conductivity. Figures 2 and 3 show profiles of DSC curves for the typical PEO–alkali metal salt complexes. The salt-free PEO network polymer and a part of the PEO–alkali metal salt complexes (PEO–LiCl, PEO–LiBr, PEO–LiSCN) showed crystallization and melting transitions in addition to glass transition. Since room temperature was somewhat higher than the melting temperatures of these samples, the profile of DSC curves looked as if the samples were quenched. The other PEO–alkali metal salt complexes showed only

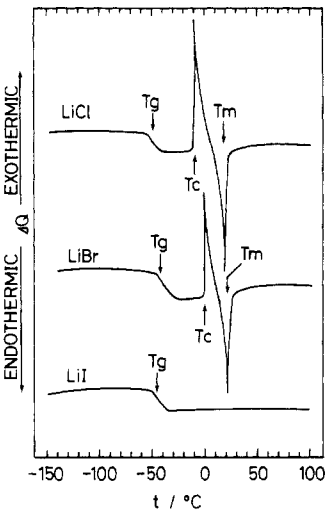

Figure 3. Profiles of DSC curves of PEO–alkali metal salt complexes.

Table I
Thermal Properties of PEO–Alkali Metal Salt Complexes

salt	T_g (zone), °C	T_c, °C	ΔH_c, J g^{-1}	T_m, °C	ΔH_m, J g^{-1}	crystallinity, %
salt free	−50 (−57 to −43)	−20	34.2	21	37.5	18.4
LiCl	−48 (−55 to −41)	−10	28.1	15	29.3	14.4
LiBr	−42 (−49 to −35)	−1	17.5	18	22.0	10.8
LiI	−45 (−51 to −39)					
LiSCN	−46 (−53 to −40)	−9	26.5	19	28.1	13.9
NaSCN	−41 (−50 to −34)					
KSCN	−43 (−49 to −37)					
$LiBF_4$	−45 (−53 to −38)					
$LiPF_6$	−41 (−46 to −36)					
$LiClO_4$	−43 (−49 to −37)					
LiPic[a]	−44 (−50 to −38)					
$LiB(Ph)_4$	−35 (−41 to −30)					

[a] Lithium picrate.

glass transition in the DSC curves, which indicated that these complexes were completely amorphous. The DSC results are summarized in Table I. The ΔH_c and ΔH_m for the PEO–LiCl, PEO–LiBr, and PEO–LiSCN complexes were represented as those per unit weight of the PEO network polymer since X-ray diffraction patterns of these complexes showed diffraction peaks at the same positions as those of the PEO network polymer. The degree of crystallinity was estimated from the ratio of the experimentally determined ΔH_m to the value of 203 J g^{-1} reported in the literature[13] for the enthalpy of melting for 100% crystalline PEO. The changes in crystallinity depending on the kinds of incorporated salts may be due to the difference in the interaction between PEO chain and the incorporated ionic species.

Figure 4 shows the temperature dependence of ionic conductivity for the completely amorphous PEO–lithium salt complexes. The temperature dependences showed continuously curved profiles, that is, WLF-type profiles, as is expected by the complexes' rubbery state in this temperature range. The conductivity at a constant temperature differed by 1 order of magnitude depending on the kind of incorporated salt and reached 10^{-5} S cm^{-1} at 30 °C and 10^{-4} S cm^{-1} at 80 °C in highly conductive complexes. Figure 5 shows the ionic conductivity of PEO–lithium halide complexes as a function of the inverse of absolute temperature. The conductivity of the PEO–LiI complex, which was amorphous from the DSC results, showed a continuously curved temperature profile, as seen in Figure 4. In contrast, the temperature profiles of conductivity for the PEO–LiBr and PEO–LiCl complexes

Table II
WLF Parameters for PEO–Alkali Metal Salt Complexes

salt	T_0, °C	C_1'	C_2', °C	$\sigma(T_0)$, S cm^{-1}	T_g, °C	C_1	C_2, °C	$\sigma(T_g)$, S cm^{-1}
LiCl	2	4.51	109.1	7.44×10^{-8}	−48	8.33	59.1	1.13×10^{-11}
LiBr	8	4.29	96.6	2.88×10^{-7}	−42	8.89	46.6	7.22×10^{-12}
LiI	5	5.00	99.0	7.02×10^{-7}	−45	10.11	49.0	5.50×10^{-12}
LiSCN	4	4.69	107.8	1.66×10^{-7}	−46	8.75	57.8	1.46×10^{-11}
NaSCN	9	4.12	77.9	9.95×10^{-7}	−41	11.49	27.9	4.16×10^{-14}
KSCN	7	4.75	80.6	8.04×10^{-7}	−43	12.51	30.6	1.41×10^{-14}
$LiBF_4$	5	4.22	86.8	8.77×10^{-7}	−45	9.96	36.8	1.59×10^{-12}
$LiPF_6$	9	4.61	82.4	1.96×10^{-7}	−41	11.37	32.4	1.48×10^{-14}
$LiClO_4$	7	4.11	78.2	7.04×10^{-7}	−43	11.40	28.2	3.57×10^{-14}
Li Pic[a]	6	4.71	124.3	4.33×10^{-7}	−44	7.88	74.3	2.92×10^{-10}
$LiB(Ph)_4$	15	4.96	113.4	1.60×10^{-7}	−35	8.87	63.4	1.48×10^{-14}

[a] Lithium picrate.

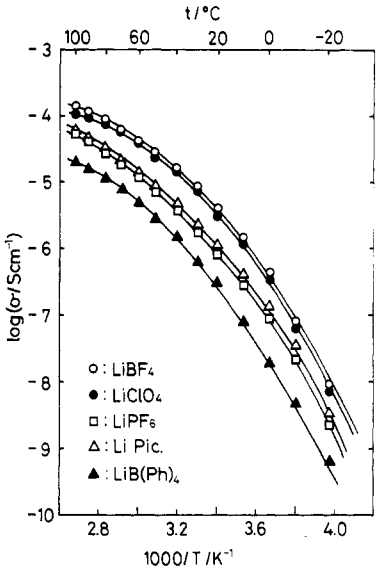

Figure 4. Temperature dependence of ionic conductivity for PEO–lithium salt complexes.

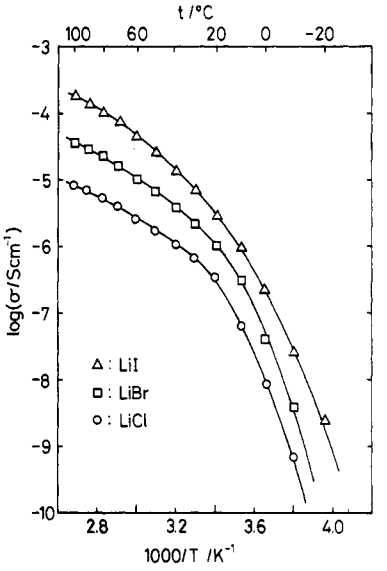

Figure 5. Temperature dependence of ionic conductivity for PEO–lithium halide complexes.

deviated negatively from the WLF profiles below 20 °C. This behavior corresponded to the crystallization of PEO segments, as seen in the DSC results. The conductivity at constant temperature decreased in the order LiI > LiBr > LiCl, which correlates with the order of the size of anion radius. Figure 6 shows the temperature dependence of conductivity for the PEO–alkali metal thiocyanates. The negative deviation of the temperature profile from the WLF-type profile was observed again in the partially crystalline PEO–LiSCN complex, whereas the amorphous PEO–KSCN and PEO–NaSCN complexes showed the WLF-type temperature profile in the whole temperature range.

The temperature dependences of ionic conductivity for the various PEO–alkali metal salt complexes in rubbery and amorphous states were fit to the following WLF-type equation:

$$\log \frac{\sigma(T)}{\sigma(T_g)} = \frac{C_1(T - T_g)}{C_2 + (T - T_g)} \tag{1}$$

In order to enhance the reliability of the estimation of WLF parameters, $T_0 = T_g + 50$ °C was selected as another reference temperature in the equation

$$\log \frac{\sigma(T)}{\sigma(T_0)} = \frac{C_1'(T - T_0)}{C_2' + (T - T_0)} \tag{2}$$

because the conductivity data close to T_g could not be measured in this experiment and further because the conductivity data above 20 °C were used for the partially

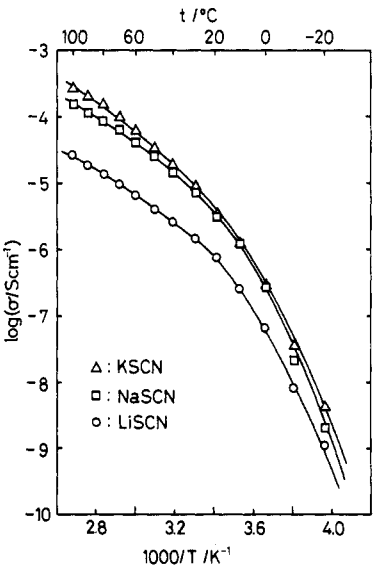

Figure 6. Temperature dependence of ionic conductivity for PEO–alkali metal thiocyanate complexes.

crystalline complexes. The parameters obtained are summarized in Table II. The parameters in eq 1 were calculated from

$$C_1 = C_1'C_2'/[C_2' - (T_0 - T_g)] \tag{3}$$

$$C_2 = C_2' - (T_0 - T_g) \tag{4}$$

and are also listed in Table II. Equations 1 and 2 with the

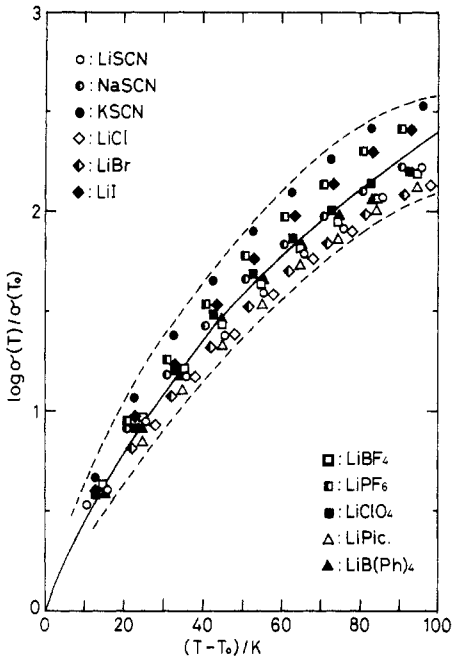

Figure 7. WLF plots of ionic conductivity for PEO–alkali metal salt complexes using a reference temperature T_0 ($=T_g + 50$ °C).

corresponding WLF parameters provided a good fit to the experimental data.

Carrier Transport and Generation Processes. Since the temperature profiles of the conductivity follow eq 1, the carrier transport process will be discussed in terms of the free volume mechanism.[14] The WLF-type equation for the diffusion coefficients of ionic carriers in rubbery and amorphous states is expressed by[9,15]

$$\log \frac{D(T)}{D(T_g)} = \frac{(\gamma V_i^*/2.303V_f)(T - T_g)}{(f_g/\alpha) + (T - T_g)} \quad (5)$$

where $D(T)$ and $D(T_g)$ are diffusion coefficients at T and T_g, respectively, γ is a factor to allow for overlap of free volume, V_i^* is the critical volume required for migration of carrier ions, V_g is the specific volume at T_g, f_g is the free volume fraction at T_g, and α is the expansion coefficient of the free volume. Ionic conductivity is expressed by

$$\sigma(T) = n(T)\mu(T)q \quad (6)$$

where $n(T)$ is the number of carrier ions per unit volume, $\mu(T)$ is the ionic mobility, and q is the charge of carrier ions. We assume that $\mu(T)$ is related to $D(T)$ by the following equation:

$$\mu(T) = qD(T)/kT \quad (7)$$

The ratio of the ionic conductivity at T to that at T_g is given by

$$\log \frac{\sigma(T)}{\sigma(T_g)} = \log \frac{n(T)D(T)T_g}{n(T_g)D(T_g)T} \simeq \log \frac{n(T)D(T)}{n(T_g)D(T_g)} \quad (8)$$

If the temperature dependence of the number of carrier ions is assumed to be negligible compared with that of the ionic mobility, eq 1 can be derived mathematically from eq 5 and 8.

Figure 7 shows WLF plots of ionic conductivity for all the PEO–alkali metal salt complexes using a reference temperature T_0 ($=T_g + 50$ °C). The WLF parameters obtained ranged from 4.1 to 5.0 for C_1' and from 78 to 124 for C_2', as seen in Table II. The conductivity values at a constant $T - T_0$ are somewhat distributed. However, this distribution was at most a half order of magnitude, which was considerably smaller than the conductivity distribution

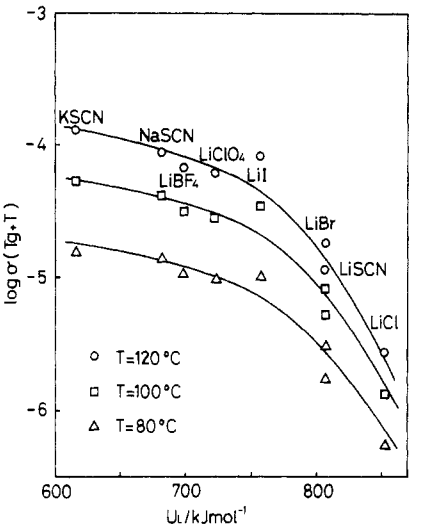

Figure 8. Ionic conductivity at constant reduced temperatures as a function of the lattice energies of incorporated salts.

of 1 or 2 order(s) of magnitude(s) at a constant temperature (see Figures 4–6). The solid line in Figure 7 is the calculated curve from eq 2, and $C_1' = 4.6$ and $C_2' = 95.6$. The parameters for this master curve were comparable to the universal values of $C_1' = 8.86$ and $C_2' = 101.6$ for the temperature dependence of the main-chain relaxation times for various kinds of amorphous polymers.[16] This fact seems to be peculiar when one realizes that the volume of carrier ion may be far smaller than that of the moving unit of PEO chain involved in the relaxation process. This may seem more reasonable when one considers that ionic migration does not occur by itself but that the segmental motion with associated carrier ions causes the ionic migration. This view has been advanced.[7,17-20] Since the moving PEO unit with associated carrier ions is far larger than the volume of naked ions and its size is nearly constant and independent of the ionic radii, one master curve for the ionic conductivity may be given irrespective of the kinds of incorporated salts. The large temperature dependence for the conduction of small ionic species is also interpreted by this consideration. The small distribution of conductivity at a constant $T - T_0$ in Figure 7 might be due to the change in the number of carrier ions with temperature, which was not taken into account in the above discussion.

The number of carrier ions changed with the kind and concentration of the incorporated salt. Figure 8 shows the ionic conductivity at constant reduced temperatures ($T_g + T$) as a function of the lattice energies[21] of the incorporated salts. The ionic mobility at these temperatures was considered to be nearly constant. Thus, changes in the conductivity with the lattice energies of the salts could be attributed to changes in the number of carrier ions. With increasing lattice energies, the conductivity tended to decrease. This indicates that all of the incorporated salt does not function as carrier ions and that the ion dissociation is suppressed with increasing lattice energies. The curvature of the relations in Figure 8 changed at a lattice energy of about 750 kJ mol^{-1}. Above this lattice energy, the decrease in conductivity became pronounced. The PEO complexes of the salts with lattice energies higher than 750 kJ mol^{-1} were partially crystalline, whereas those with lower lattice energies were completely amorphous, as seen from Table I. This indicates that the interaction of ions with the ether oxygen atoms in the PEO chain is an essential process for the carrier generation, and this interaction inhibits the crystallization of PEO chain. Figure

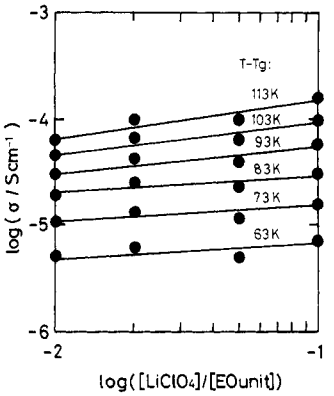

Figure 9. Ionic conductivity as a function of salt concentration for PEO–$LiClO_4$ complexes.

9 shows the ionic conductivity of the PEO–$LiClO_4$ complexes as a function of the salt concentration at constant reduced temperatures. The increase in the conductivity with the concentration was smaller than that expected by the complete dissociation. This also indicates that all of the incorporated salt does not function as carrier ions. The formation of ion pairs and other aggregates seems to occur at a higher concentration. We cannot deny at the present the possibility of long-range ion interaction which reduces the ionic mobility at constant reduced temperatures with increasing salt concentration.

References and Notes

(1) See, for instance: *Solid State Ionics* **1986**, *18/19*, 253–347 (Proceedings of the 5th International Conference on Solid State Ionics).
(2) Hooper, A.; North, J. M. *Solid State Ionics* **1983**, *9/10*, 1161.
(3) Gauthier, M.; Fauteux, D.; Vassort, G.; Belanger, A.; Duval, M.; Ricoux, P.; Chabagno, J. M.; Muller, D.; Rigaud, P.; Armand, M. B.; Deroo, D. *J. Electrochem. Soc.* **1985**, *132*, 1333.
(4) Wright, P. V. *Br. Polym. J.* **1975**, *7*, 319.
(5) See, for instance: Minier, M.; Berthier, C.; Gorecki, W. *J. Phys.* **1984**, *45*, 739.
(6) Armand, M. B.; Chabagno, J. M.; Duclot, M. J. In *Fast Ion Transport in Solids*; Vashishta, P., Mundy, J. N., Shenoy, G. K., Eds.; North-Holland: New York, 1979; pp 131–136.
(7) Killis, A.; LeNest, J. F.; Cheradame, H.; Gandini, A. *Makromol. Chem.* **1982**, *183*, 2835.
(8) Killis, A.; LeNest, J. F.; Gandini, A.; Cheradame, H. *Macromolecules* **1984**, *17*, 63.
(9) Watanabe, M.; Nagano, S.; Sanui, K.; Ogata, N. *Solid State Ionics* **1986**, *18/19*, 338.
(10) Watanabe, M.; Nagano, S.; Sanui, K.; Ogata, N. *Polym. J. (Tokyo)* **1986**, *18*, 809.
(11) Watanabe, M.; Sanui, K.; Ogata, N.; Inoue, F.; Kobayashi, T.; Ohtaki, Z. *Polym. J. (Tokyo)* **1984**, *16*, 711.
(12) Watanabe, M.; Rikukawa, M.; Sanui, K.; Ogata, N.; Kato, H.; Kobayashi, T.; Ohtaki, Z. *Macromolecules* **1984**, *17*, 2902.
(13) Wunderlich, B. In *Macromolecular Physics*; Academic: New York, 1980; Vol. 3, p 67.
(14) Cohen, M. H.; Turnbull, D. *J. Chem. Phys.* **1959**, *31*, 1164.
(15) Watanabe, M.; Sanui, K.; Ogata, N.; Kobayashi, T.; Ohtaki, Z. *J. Appl. Phys.* **1985**, *57*, 123.
(16) Williams, M. L.; Landel, R. F.; Ferry, J. D. *J. Am. Chem. Soc.* **1955**, *77*, 3701.
(17) Wong, T.; Brodwin, M.; Papke, B. L.; Shriver, D. F. *Solid State Ionics* **1981**, *5*, 689.
(18) Watanabe, M.; Sanui, K.; Ogata, N. *Macromolecules* **1986**, *19*, 815.
(19) Watanabe, M.; Suzuki, A.; Sanui, K.; Ogata, N. *Nippon Kagaku Kaishi* **1986**, 427.
(20) Watanabe, M.; Suzuki, A.; Santo, T.; Sanui, K.; Ogata, N. *Macromolcules* **1986**, *19*, 1921.
(21) Jenkins, H. D. B.; Waddington, T. C. In *The CRC Handbook of Chemistry and Physics*; Chemical Rubber: Cleveland, OH, 1980–1981; Vol. 61.

Sequence Distributions and a Phase Diagram for Copolymers Made from Poly(ethylene terephthalate) and *p*-Acetoxybenzoic Acid

V. A. Nicely,* J. T. Dougherty, and L. W. Renfro

Research Laboratories, Eastman Chemicals Division, Eastman Kodak Company, Kingsport, Tennessee 37662.

Received June 9, 1986

ABSTRACT: Copolymers made from poly(ethylene terephthalate) (PET) and *p*-acetoxybenzoic acid (PHB) have been examined in solution and as melts by NMR spectroscopy. Proton and carbon NMR spectra of solutions have shown that the sequence distributions for PET/PHB copolyesters can be described in terms of a probability model in which PHB has a slightly greater than random chance of being bonded to another PHB, which leads to significant deviations from randomness at higher PHB levels in the copolymer. Proton wide-line NMR spectra on melts show evidence of both liquid crystalline and isotropic phases for compositions at or above 35 mol % PHB. The compositions of the isotropic and anisotropic phases are found to contain approximately 35 and 80 mol % PHB, respectively, at 280 °C. The amount of each phase is estimated for several compositions up to 80 mol % PHB. A qualitative explanation of the formation of the liquid crystalline phase requires significant amounts of sequences of four or more PHB units to initiate liquid crystalline phase formation. At compositions with enough PHB to separate a liquid crystalline phase, shorter sequences of PHB partition between the phases to enrich further the PHB-rich phase.

Introduction

The series of copolyesters based upon poly(ethylene terephthalate) that has been copolymerized with *p*-acetoxybenzoic acid has been the subject of several investigations into their structure and properties. The copoly(ethylene terephthalate/*p*-oxybenzoyl) copolyesters, called PET/PHB, have been shown to exhibit liquid crystallinity at or above 35 mol % PHB.[1] The PET/60PHB and PET/80PHB copolyesters, having 60 and 80 mol % *p*-oxybenzoyl moieties, respectively, are reported to show domains,[2–5] and to have thermal properties[2,3,5,6] and diffraction patterns[2,4,7,8] domains[2–5] with phase separation into PHB- and PET-rich phases in their solids. Although the copolyesters have been reported to be random copolyesters based upon ^{13}C NMR spectra,[1,9] the phase separation[2,5] and morphology results[2,5] have been interpreted as evidence for blocked sequence distributions in these copolymers.

The NMR evidence for chain sequence statistics has been reexamined with a high-field spectrometer. It provides better sensitivity for carbon results and proton re-

0024-9297/87/2220-0573$01.50/0